

Synthesis and Characterization of Hierarchical Metallosilicate Macrospherical Catalysts

EMIL IOAN MURESAN^{1*}, VASILICA POPESCU², ION SANDU^{3,4}

¹Gheorghe Asachi Technical University, Department of Organic and Biochemical Engineering, Faculty of Chemical Engineering and Environment, Management, 73 Blvd. Dimitrie Mangeron, Iasi-700050; Romania

²Gheorghe Asachi Technical University, Faculty of Textiles, Leather Engineering and Industrial Management, 29 Blvd. Mangeron, TEX 1 Building, Iasi 700050, Romania

³Alexandru Ioan Cuza University, ARHEOINVEST Interdisciplinary Platform, Carol I, no. 11, Corp G demisol, 700506, Iasi, Romania

⁴Romanian Inventors Forum, Sf. P. Movila 3, Str. L11, III/3, 700089, Iasi, Romania

This work reports an original method for the obtaining of hard macrospherical metallosilicate catalysts. Due to their sizes and hardness these catalysts are easy to recover and to reuse. Porous metallosilicate microspheres (0.9÷1.1 mm) that contain chromium (III) ions as main active catalytic centers were easily synthesized at room temperature using tetraethyl orthosilicate as silicon source and chitosan as template and shape generating agent. Three starting silicon/metals molar ratios and three chitosan/TEOS ratios were used for the synthesis of catalysts. The concentration of chitosan from the synthesis gel influenced the porosity, the size and the shape of catalyst particles. The synthesized catalysts were characterized by water sorption isotherms, FTIR spectroscopy, DR UV-vis and EDX analyses. Catalytic activity and the reusability of the catalyst were tested for the addition reaction of caprylic acid to epichlorohydrin. This new synthesis method of hard porous metallosilicate microspheres encourages the replacement of homogeneous catalysts with their heterogeneous counterparts.

Keywords: hard metallosilicate microspheres, heterogeneous catalysis, hierarchical micro/meso/macroporous materials

In the recent years synthesis of hierarchical metallosilicate materials using templating method has received much attention. Interconnected metallosilicate network is generated by hydrolysis and condensation reactions of the precursor material that covers and fills the template structure. Once the precursor has reacted, the subsequent removal of the template gives the hierarchical porous structure. Materials with hierarchical porosity combine the advantages of high surface area (due to the presence of micro and mesopores) with the increased mass transport due to the presence of macropores.

Until now various routes for the synthesis of hierarchical metallosilicate materials have been reported, but there is only a limited number of works that approach the obtaining of macroscopic shape zeolites [1-15]. The materials that combine micro/meso/macroporous structure with the controlled size and shape of particles are attractive heterogeneous catalysts for industrial applications. Particularly spherical form is often preferable for catalytic applications due to limited attrition and easy handling. Hierarchical macrospherical beads avoid the main drawback of metallosilicate catalysts in the form of nano and microparticles related to awkward separation from the reaction mixture during catalyst recycling (which normally requires high speed centrifugation or special filtration). On the other hand, by incorporation of transitional metals into the silica framework is avoided the leaching of active metallic ions under the reaction conditions [16-20]. The use of heterogeneous catalysts instead of their homogeneous counterparts became a prime target in green chemistry because they are environmentally friendly and allow the reuse of incorporated metals.

Starting from previously achievements in the field of heterogeneous catalysis and taking into account the current stage of researches regarding the addition of carboxylic acids to oxyranes we proposed to synthesize new materials that contain Cr³⁺ ions that exhibit high catalytic activity in the esterification reaction of carboxylic acids with oxyranes.

This study reports a general method for incorporation of metals within the silica framework. By this new synthesis route one obtains macrospherical heterogeneous catalysts that can be easily separated from the reaction mixture and recycled. Hierarchical micro/meso/macro porous tetrametallosilicate microspheres presented in this work were obtained by incorporation of four metallic ions (Cr, Al, Zr and Zn) within the silica matrix using tetraethyl orthosilicate as silicon source and chitosan as template and shape generating agent. Chromium ions represent the main active catalytic centers, while the others metals are especially intended to increase the mechanical strength of the catalyst beads. The chemical, thermal and mechanical stability as well as the possibility of being reused make the porous metallosilicate beads promising heterogeneous catalysts. Catalytic activity and recyclability of the macrobeads were tested in the esterification reaction of caprylic acid with epichlorohydrin.

Experimental part

Materials and methods

The reactives used for synthesis include aluminium chloride (AlCl₃·6H₂O, Aldrich), chromium nitrate (Cr(NO₃)₃·9H₂O, Aldrich), zirconium oxychloride (ZrOCl₂·8H₂O, Aldrich), zinc chloride (ZnCl₂, Aldrich), (HCl 37%, Aldrich) ammonium solution 25%, tetraethyl

* email: eimuresan@yahoo.co.uk

orthosilicate (TEOS, Aldrich), chitosan with high molecular weight (Aldrich), cetyltrimethylammonium bromide (CTAB, Aldrich). For the esterification reaction were used epichlorohydrin 99% (Aldrich) and caprylic acid 99% (Aldrich). All the chemicals were used as received.

Synthesis of the metallosilicate beads

For the preparation of metallosilicate macrospheres 4g of chitosan with high molecular weight was dissolved in acetic acid solution (4% v/v) to form 4% solution (w/v). The chitosan solution was left overnight to ensure that all of the chitosan was dissolved. HCl (37%) solution, CTAB, $\text{Cr}(\text{NO}_3)_3 \cdot 9\text{H}_2\text{O}$, $\text{ZrOCl}_2 \cdot 8\text{H}_2\text{O}$, $\text{AlCl}_3 \cdot 6\text{H}_2\text{O}$ and anhydrous ZnCl_2 were dissolved in distilled water. To this solution TEOS was added under stirring. The molar composition of the synthesis gel was: 1.00 $\text{Cr}(\text{NO}_3)_3 \cdot 9\text{H}_2\text{O}$: 1.00 $\text{ZrOCl}_2 \cdot 8\text{H}_2\text{O}$: 0.67 $\text{AlCl}_3 \cdot 6\text{H}_2\text{O}$: 0.67 ZnCl_2 : x TEOS : 0.034x CTAB : 0.30 x HCl : 48x H_2O , where x = 0.055; 0.046 and 0.027. The mixture was vigorously stirred at room temperature for 6 hours. Subsequently chitosan solution 4% (w/v) was added to the above mixture. The mole ratio chitosan/TEOS was 0.14 : 1.00 in the experiments where the effect of TEOS/metals mole ratio was studied, and took the values 0.14 : 1.00, 0.17 : 1.00 and respectively 0.20 : 1.00 in the experiments wherein the effect of chitosan/TEOS mole ratio was investigated. After another 40 min of energetically stirring the gel was added dropwise with a syringe pump into a precipitation bath containing an ammonia solution (25% v/v). Hybrid macrospheres are formed in situ when drops of chitosan containing the gel fall down in concentrated ammonia solution. The sprayed particles were kept into ammonia coagulating solution (to harden) for 45 min. The obtained macrospheres were separated by filtration in a Buchner funnel and then dried at 50°C for 12 h. The dried samples were calcinated in air at 615°C for 14 h (increasing the temperature with a heating rate of 2°C/min) for removal of the template.

In order to remove the non-framework metallic ions the calcined samples were washed with distilled water (90°C), then with 1M ammonium acetate solution (90°C).

For comparative study macrospheres of silica (denoted as Si) with a composition similar to that of catalyst C_1 (the same amounts of TEOS, HCl, CTABr and chitosan but without adding of metallic salts) were also synthesized.

Characterization of the synthesized materials

The FTIR spectra were performed with the FTIR spectrometer Vertex 70 (Bruker) using the conventional KBr-disk technique. Infrared spectrum in the range 4000 - 400 cm^{-1} was obtained by the co-addition of 32 scans with a resolution of 2 cm^{-1} .

The diffuse reflectance UV-visible spectra were measured with a Shimadzu UV-2450 spectrophotometer equipped with an integrating sphere assembly. All the spectra were recorded against barium sulphate in the 190 ÷ 800nm wavelength range and plotted in terms of absorbance.

Scanning electron microscopy with X-ray microanalysis (SEM/EDX) was carried out with Quanta 200 (Fei) scanning electron microscope coupled with an energy dispersive X-ray analyzer. Samples were prepared by dispersing dry powder shell on copper support and coated with gold by cathode deposition using an EMITECHK 550 apparatus.

Water adsorption-desorption isotherms were recorded on an automated gravimetric analyzer IGAsorp produced by Hiden Analytical, Warrington (UK). One of the most important parts of this equipment is an ultrasensitive microbalance which measures the weight change as the

humidity is modified in the sample chamber at a constant regulated temperature. System measurements are fully automated and controlled by a software package. Before sorption measurement the sample was dried at 25°C in flowing nitrogen (250 cm^3/min) until the weight of the sample was in equilibrium at $\text{RH} < 1\%$. Then the relative humidity (RH) was gradual increased from 0 to 90%, in 10% humidity steps, everyone having a pre-established equilibrium time between 5 and 10 min and the sorption equilibrium was obtained for each step. After that, the RH decreased and desorption curves were registered.

Catalytic activity of metallosilicate beads in the addition reaction of caprylic acid to epichlorohydrin

Esterification reaction was carried out in a three-necked glass flask equipped with a reflux condenser, a sample device and a thermocouple. The temperature was controlled within $\pm 0.5^\circ\text{C}$ by a thermostating bath. A magnetic stirrer was used to mix the reactants. The frequency of stirring was 500 rpm. Caprylic acid and epichlorohydrin were loaded into the reactor and then heated to the desired temperature. Finally a given amount of catalyst was added. This was taken as the zero time of reaction. The amount of unreacted acid from the samples withdrawn at regular time periods was determined by titration against a standard alcoholic solution of 0.1 M NaOH using phenolphthalein as indicator.

Results and discussions

Taking into account the high catalytic activity of chromium in the reaction of carboxylic acids with epichlorohydrin as well as the advantages of heterogeneous catalysis one attempted the synthesis of catalyst macrospheres that contain chromium incorporated within a polymer matrix of TEOS. In order to get macrospheres, chitosan (a substance that coagulate in alkaline media) was used. Chitosan fulfills both the role of shape generating agent as well as the role of template for the synthesized materials.

Preliminary experiments showed that the macrospheres obtained only by incorporating of chromium within the silica network do not present a satisfactory mechanical strength. Therefore other metals were added into the silica matrix in order to increase the mechanical strength of the catalyst beads. Mechanical strength studies performed with a digital dynamometer for compression lead to the conclusion that the best results were obtained by incorporation of four metals (Cr, Al, Zr and Zn) in the polymeric matrix of TEOS (table 1).

Sample 8 obtained by incorporation of the four metals within the silica matrix presents the best mechanical strength (3.75N corresponding to 4.7MPa).

Synthesis of the catalysts

Taking into account the previously mentioned results our researches focussed on the synthesis of macrospherical catalysts that contain four metals incorporated within the silica framework. The composition of mixtures used for the synthesis of catalysts (according to the method presented in the experimental part) is shown in table 2. The amount of metals was kept constant in all the experiments. In order to study the influence of the TEOS/metal ratio one worked with three molar ratios TEOS/metal (catalyst C_1 , catalyst C_2 and catalyst C_3). Influence of the chitosan/TEOS ratio was studied in the case of catalyst C_1 , catalyst C_4 and respectively catalyst C_5 . The amount of water added for each experiment was calculated so that the chitosan concentration in the reaction mixture was 1.30% (w/v).

Sample no.	Molar composition of the catalyst					Crush strength ^a (N)
	Si	Cr	Zr	Al	Zn	
1	1.000	0.183	-	-	-	0.10
2	1.000	0.092	-	0.092	-	0.12
3	1.000	0.092	-	-	0.092	0.21
4	1.000	0.092	0.092	-	-	2.52
5	1.000	0.061	0.061	0.061	-	1.84
6	1.000	0.061	-	0.061	0.0601	0.18
7	1.000	0.061	0.061	-	0.061	2.86
8	1.000	0.055	0.055	0.037	0.037	3.75

^a Crush strength was determined for macrospheres with mean diameter of 1 mm.

Table 1
MECHANICAL STRENGTH FOR
DIFFERENT SAMPLES

Catalyst composition	Catalyst C ₁	Catalyst C ₂	Catalyst C ₃	Catalyst C ₄	Catalyst C ₅	Silica macro-spheres Si
Cr(NO ₃) ₃ ·9H ₂ O, (g)	0.4416	0.4416	0.4416	0.4416	0.4416	-
AlCl ₃ ·6H ₂ O, (g)	0.1777	0.1777	0.1777	0.1777	0.1777	-
ZrOCl ₂ ·8H ₂ O, (g)	0.3555	0.3555	0.3555	0.3555	0.3555	-
ZnCl ₂ , (g)	0.1000	0.1000	0.1000	0.1000	0.1000	-
CTMABr, (g)	0.2490	0.2075	0.1245	0.2490	0.2490	0.249
Water, (mL)	18.3000	15.2000	9.2000	23.0000	27.6000	18.300
HCl 37%, (mL)	0.6000	0,5000	0.3000	0.6000	0.6000	0.600
TEOS, (mL)	4.5000	3.7500	2.2500	4.5000	4.5000	4.500
CHT 4%, (g)	11.2500	9.3750	5.6250	13.5000	15.7500	11.2500

Table 2
COMPOSITION OF THE SYNTHESIS
MIXTURES

Effect of the chitosan concentration on the shape and the size of particles

The concentration of the chitosan from the synthesis gel influences the shape and the size of the particles (fig. 1).

Gels with a content of chitosan in the range $0.90 \div 1.25\%$ (w/v) are less viscous, but the macrospheres resulted by their coagulation, drying and calcination have smaller sizes (mean diameter 0.63mm) and lower porosities (fig. 1a). By using a chitosan concentration higher than 1.35% (w/v) one obtains more viscous gels that results in larger particles (mean diameter 1.41mm) that no longer have a perfect spherical shape (fig. 1c). Chitosan concentrations between $1.25 \div 1.35\%$ (w/v) are suitable for manufacture of large spherical particles (mean diameter 1.02mm) with good catalytic activity (fig. 1b). Considering the foregoing one worked in this study with a chitosan concentration of 1.30% (w/v) which allows the incorporation of large amounts of metals in the silicon matrix and also obtaining of macrospheres with higher porosities.

EDX analyses

The influence of TEOS/metals ratio and respectively the effect of chitosan/TEOS ratio on the effectiveness of metal incorporation within the silica framework were estimated from the composition of the synthesized catalysts determined by EDX analyses of the catalysts (table 3).

From the experimental results one notices that the best incorporation of metals within the silica framework was obtained for C₃ and C₂ catalysts. For these catalysts the ratios chitosan/TEOS were 0.12g chitosan/1cm³ TEOS and respectively 0.1g chitosan/1cm³ TEOS.

Water adsorption-desorption isotherms

The water adsorption-desorption isotherms and the pore size distribution curves of the synthesized catalysts are shown in figure 2.

Adsorption and desorption isotherms were measured over a range of relative pressures p/p_0 from 0.00 to 0.85. The amount of water adsorbed at $p/p_0 = 0.85$ gives an estimate of the total volume of accessible micro and mesopores in the catalyst. According to IUPAC classification, the adsorption/desorption isotherms of synthesized materials can be associated to type V curves describing sorption on hydrophobic/low hydrophilic materials with weak sorbent-water interactions, with low sorption at low RH and sometimes moderate sorption at the middle RH and suddenly high water sorption at RH close to 100 [21-23]. The occurrence of plateau with hysteresis is related to the presence of mesopores. In figure 2 one can see that the final mass is not the same with the initial one, because a small part of the adsorbed water remains in it.

The water adsorption data were modeled using the BET method that accounts for multilayer adsorption. The specific surface areas a_s of the catalysts were calculated according to the following equation:

$$a_s = \frac{V_m N_A \sigma}{22,414 \cdot m} = \frac{M_m N_A \sigma}{\rho \cdot 22,414 \cdot m} \quad (1)$$

where: V_m is the volume necessary to cover the surface of the catalyst with a complete monolayer of gas molecules; M_m is the mass of monolayer, ρ is the density of liquid water at the temperature to which the experiment is carried out, N_A is the Avogadro number, σ is the cross-sectional

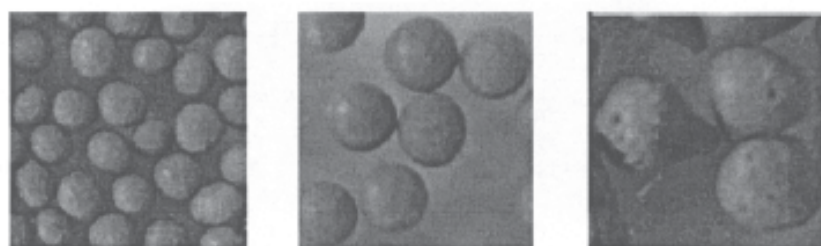


Fig. 1. The effect of chitosan concentration on the shape and the size of particles

Element	C1		C2		C3		C4		C5	
	Wt%	At%								
C	11.34	20.5	11.15	22.42	13.11	24.68	10.70	19.14	9.89	17.40
N	1.88	2.58	1.91	2.66	1.94	2.76	1.80	2.52	1.70	2.45
O	39.33	49.77	35.59	47.06	33.37	43.9	39.91	50.98	40.65	52.53
Na	0.31	0.25	0.35	0.29	0.39	0.33	0.28	0.22	0.24	0.18
Al	1.16	0.77	1.53	1.08	1.97	1.43	1.12	0.74	1.07	0.71
Si	34.42	22.99	34.02	21.74	29.2	20.29	35.02	23.37	35.78	23.85
Zr	5.82	1.24	7.84	2.10	10.21	3.09	5.63	1.20	5.39	1.16
Cr	3.33	1.19	4.41	1.66	5.68	2.21	3.21	1.15	3.05	1.09
Zn	2.41	0.71	3.20	0.99	4.13	1.31	2.33	0.68	2.23	0.63

Table 3
ELEMENTAL COMPOSITION OF THE CATALYSTS

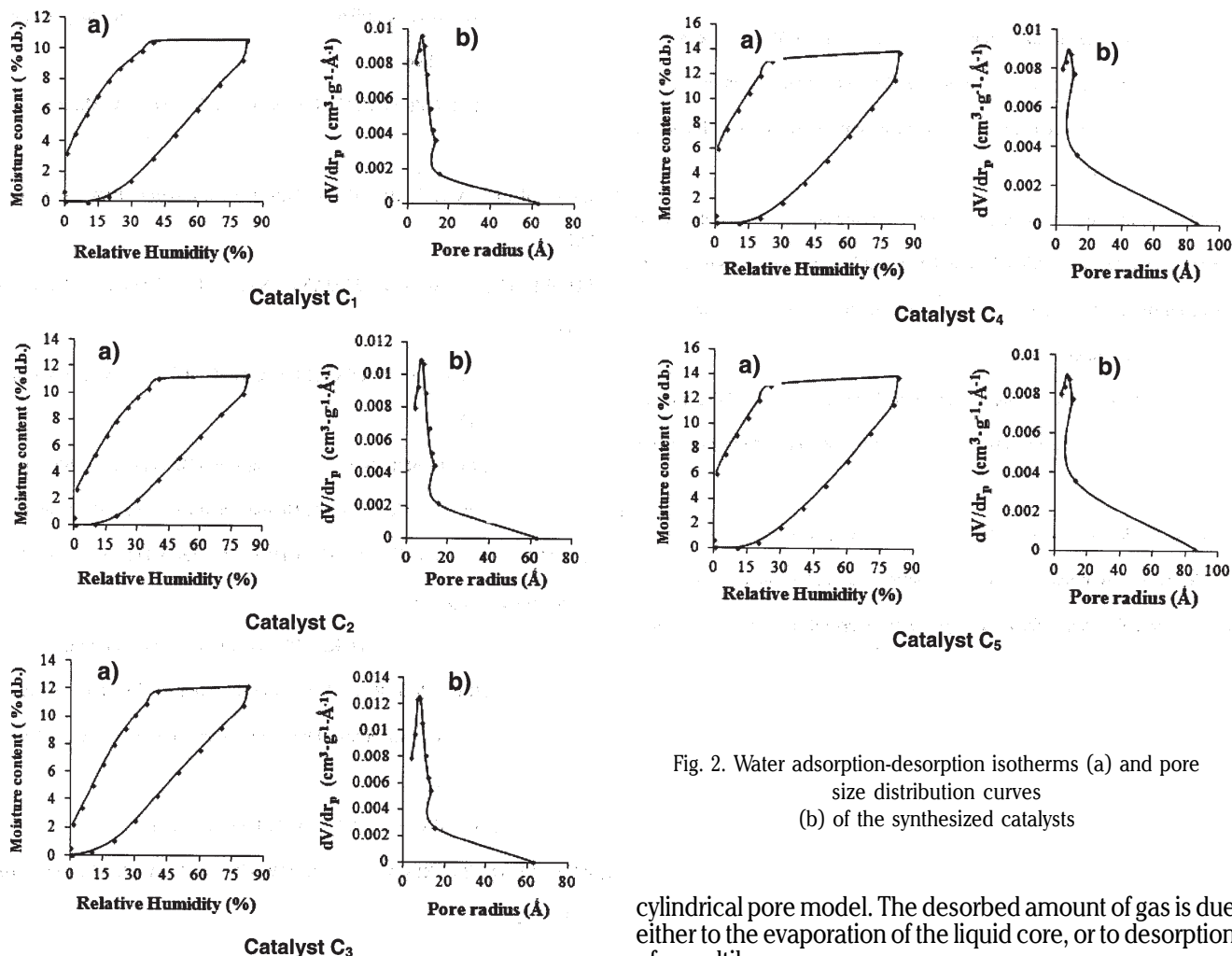


Fig. 2. Water adsorption-desorption isotherms (a) and pore size distribution curves (b) of the synthesized catalysts

area of the probe molecule (for water $\sigma = 12.5 \text{ \AA}^2$ /molecule), $22,414 \text{ cm}^3$ is the molar volume of gas at standard temperature and pressure, m is the weight of the sample.

The value of the monolayer mass M_m is obtained from the application of BET equation to the desorption branch of the isotherm data in the relative pressure range $0.01 < p/p_0 < 0.35$:

$$\frac{p}{M \cdot (p_0 - p)} = \frac{1}{C \cdot M_m} + \frac{C-1}{M_m \cdot C} \cdot \frac{p}{p_0} \quad (2)$$

respectively:

$$\frac{RH}{M \cdot (1 - RH)} = \frac{1}{C \cdot M_m} + \frac{C-1}{M_m \cdot C} \cdot RH \quad (3)$$

where M is the amount of water vapours adsorbed at equilibrium pressure (p) and C is a constant exponentially related to the enthalpy of adsorption (BET constant).

The pore size distribution was determined from the desorption branch of the isotherm according to the BJH (Barret, Joyner and Halenda) method assuming a straight

cylindrical pore model. The desorbed amount of gas is due either to the evaporation of the liquid core, or to desorption of a multilayer.

The apparent pore radius at which capillary evaporation takes place is calculated from the Kelvin equation:

$$r_K = \frac{2 \cdot \gamma \cdot V}{R \cdot T \cdot \ln(p/p_0)} \quad (4)$$

where: p – equilibrium vapour pressure of adsorbate; p_0 – saturation vapour pressure of adsorbate; p/p_0 – relative pressure of adsorbate (RH – relative humidity); γ – is the surface tension of the wetting liquid at 300K; V – molar volume of the liquid water at 300K; R – is the universal gas constant; T – absolute temperature at which the adsorption/desorption experiments were recorded.

The real pore radius (which is larger than the apparent one due to the presence of the multilayer adsorbed film at the surface having thickness t) was estimated with the corrected Kelvin equation $r_p = r_K + t$ where t is the thickness of the multilayer adsorbed film.

Pore size distribution (fig. 2b) is represented by plotting the derivative of the pore volume with respect to pore radius (dV/dr_p) against the pore radius, r_p (Å).

The average pore size estimated by the BJH model was calculated using the following equation: $r_{pm} = 2 \cdot V_{liq}/A$ where r_{pm} is the average pore size (for micro and mesopores), A is the BET surface area, and V_{liq} is the liquid volume. The relationship between the liquid volume V_{liq} and the amount of uptaken water is: $V_{liq} = M_w/\rho_w$, where: M_w – is the mass of adsorbed water, ρ_w – is the density of the liquid water.

The values of structural parameters derived from water sorption isotherms for all the samples are presented in the table 4.

As the gas sorption isotherm technique usually covers the pore size range less than 3000Å, the pycnometric methods were carried out in order to determine the total pore volume of catalyst beads [24-26]. The total pore volume (V_p) was estimated with the following equation:

$$V_p = \frac{1}{\rho_{ap}} - \frac{1}{\rho_r} \quad (5)$$

where: ρ_{ap} is the apparent density and ρ_r is the real density.

The average pore radius r_p (that considers the contributions of all three types of pores: micro, meso and macropores) was calculated with the equation [27]:

$$r_p = \frac{2 \cdot V_p}{A} \quad (6)$$

The values of total pore volume, porosity and respectively the average pore size (for micro, meso and macropores) calculated for all the five catalysts are shown in table 5.

Both the molar ratio silicon/metal as well as the amount of chitosan introduced in the synthesis gel influence the textural properties of the catalysts (table 4 and 5). A higher ratio of metal/silica (catalyst C_1 , catalyst C_2 and catalyst C_3) leads to a slight increase of micropore and mesopore volume. By using a higher amount of chitosan (catalyst C_4 , catalyst C_5) increases the porosity of the catalyst due to the increase of the meso and macropore volume.

FTIR analysis

FTIR spectra of the catalysts C_1 , C_3 and C_5 are compared with that of the silica sample (fig. 3).

The broad band around 3447 ÷ 3464 cm^{-1} was attributed to -OH stretching vibrations of adsorbed water molecules overlapped with -OH stretching vibrations of surface silanols. The peaks at 1638 ÷ 1640 cm^{-1} were assigned to the bending mode vibrations of adsorbed water molecules. The peaks at 459 ÷ 464 cm^{-1} are assigned to the bending

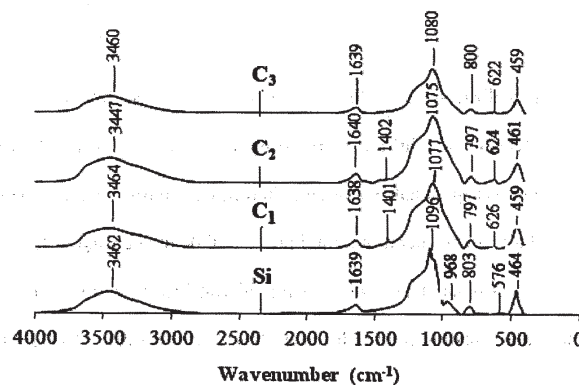


Fig. 3. FTIR spectra for Si, C_1 , C_2 and C_3 materials

mode vibrations of Si – O – Si bonds (in the case of silica sample), or to overlapping of bending mode vibrations of Si – O – Si bonds with those of Si-O-M bonds (in the case of catalysts samples). The symmetric stretching vibrations of Si-O-Si bonds occur at 797 ÷ 803 cm^{-1} , while the peaks of asymmetric stretching vibrations of Si-O-Si bonds occur at 1075 ÷ 1096 cm^{-1} . The shifts of the lattice vibration bands to lower wave numbers are due to substitution of silicon by metal ions. The adsorption band at 968 cm^{-1} (Si spectrum) is referred to the stretching vibrations of the free silanol Si-OH groups on the surface of the solid samples. The disappearance of this peak in the others spectra proves the incorporation of metallic ions within the polymeric matrix by formation of coordinative covalent bonds M-O. The signal detected at 576 cm^{-1} (Si spectrum) is due to rocking vibrations of Si-O-Si bonds; disappearance of this peak from the other spectra is due to hardening of polymer matrix by insertion of metallic ions. The signal detected at 622 ÷ 626 cm^{-1} is assigned to stretching vibrations of Si-O-M bonds [28-30].

The formation of Si-O-M bonds is further confirmed by the changes that occur in the Far-Infrared spectra (fig. 4).

Analyzing the Far-IR spectra of the silica and catalyst C_3 samples one notices that the band at 464 cm^{-1} of the catalyst sample (that aggregates the contributions of formed Si-O-M and Si-O-Si bonds) is enhanced (broader and higher) compared to the absorption band at 455 cm^{-1} of the silica sample due to partial substitution of Si-O-Si bonds with Si-O-M bonds (the signals of Si-O-M bonds are stronger than the signal of Si-O-Si bonds). The coordination of metallic cations to oxygen is also confirmed by the appearance of characteristic absorption bands at 185 and 214 cm^{-1} .

Sample	Average pore size (nm)	V pore		BET	
		$V_{micropores}$ ($cm^3 \cdot g^{-1}$)	$V_{mezopores}$ ($cm^3 \cdot g^{-1}$)	Area ($m^2 \cdot g^{-1}$)	Monolayer (g/g)
C_1	0.904	0.025	0.082	236.494	0.0673
C_2	0.876	0.026	0.088	260.085	0.0740
C_3	0.855	0.027	0.096	287.778	0.0819
C_4	0.865	0.025	0.098	284.555	0.0831
C_5	0.815	0.024	0.115	340.861	0.1010

calculated for micro and mesopores

Table 4
TEXTURAL PROPERTIES OF THE CATALYST BEADS

Pore characteristic values	Catalyst C_1	Catalyst C_2	Catalyst C_3	Catalyst C_4	Catalyst C_5
Total pore volume ($cm^3 \cdot g^{-1}$)	0.400	0.405	0.411	0.446	0.497
Average pore size (nm^{-1})	3.382	3.140	2.856	3.163	2.916

calculated for micro, meso and macropores

Table 5
TOTAL VOLUME AND AVERAGE PORE SIZE

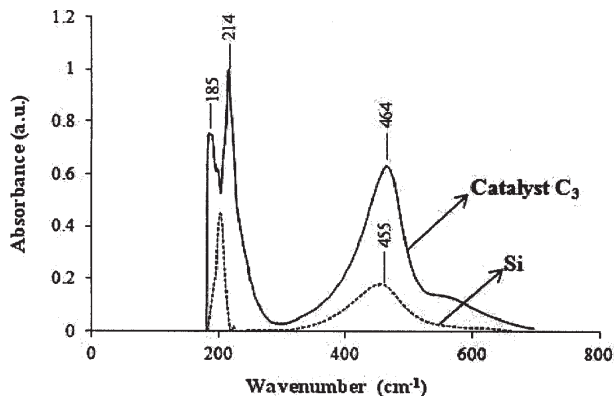


Fig. 4. Far-IR spectra of the catalyst C_3 and silica samples

Diffuse reflectance UV-Vis analysis

The DR UV-Vis spectroscopy is a technique usually used to distinguish the presence of transition metal ions within the silica framework. In order to study the influence of calcination on oxidation state of Cr(III) ions the UV-Vis spectra of uncalcined C_3 catalyst (only dried), calcined C_3 catalyst and recalculated C_3 catalyst (after the fourth reuse) were performed (fig. 5).

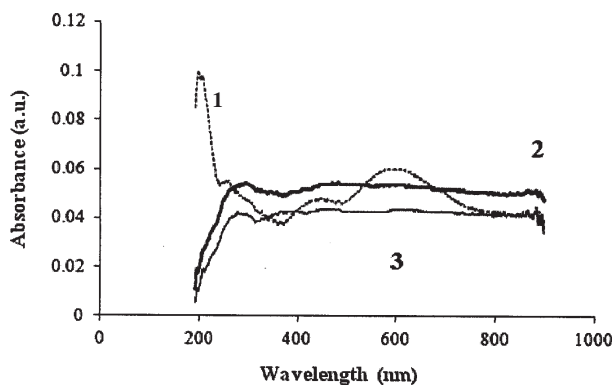


Fig. 5. DR/UV-vis spectra of catalyst C_3 : (1) dried catalyst, (2) calcined catalyst – not used in reaction, (3) recalculated catalyst (after the fourth reuse)

The DRUV-Vis spectra of dried C_3 catalyst (spectrum 1) shows four absorption bands: first band with maximum at 197nm sums up the contribution of signals from the chitosan, aluminum, zirconium and zinc, while the peaks from 253, 445 and respectively 598nm are assigned to Cr(III). The disappearance of the bands located at 445 and 598nm (spectrum 1) from the spectra of calcined catalyst (spectrum 2 and spectrum 3) can be explained by incorporation of chromium ions within the silica matrix during calcinations of macrospheres, while the disappearance of peak from 197nm (spectrum 1) is due to removal of chitosan by calcination. The charge transfer $O \rightarrow M$ absorption bands of the four metals are overlapped and form a single broad band centered around 283nm (spectrum 2) and 290nm (spectrum 3). The DR/UV-Vis spectra of chromium containing catalyst after the fourth reuse (spectrum 3) shows distinctive charge transfer $O \rightarrow Cr$ absorption bands at approximately 290, 445 and 642nm typical for Cr(III) ions in octahedral coordination. The lack of absorption bands at about 350 and 240 nm

Catalyst composition	Si (mole)	Metals(mole)			
		Al	Zr	Cr	Zn
After first reuse	1	0.070	0.108	0.105	0.061
After fourth reuse	1	0.070	0.108	0.105	0.061

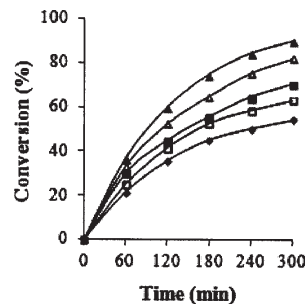


Fig. 6. The time dependence of caprylic acid conversion: \blacktriangle - Catalyst C_3 , \triangle - Catalyst C_2 , \blacksquare - Catalyst C_5 , \square - Catalyst C_4 , \blacklozenge - Catalyst C_1 . (molar ratio caprylic acid : epichlorohydrin = 1.00:1.15; stirring speed 500 r.p.m.; catalyst loading = 15g catalyst/100g reaction mixture; 85°C)

characteristique to Cr(VI) proves that chromium ions does not change their oxidation state by calcination [28-32].

Catalytic tests

Catalytic activity of the synthesized materials was tested in the addition reaction of caprylic acid to epichlorohydrin (fig. 6).

The various number of active centers (various number of chromium III ions incorporated within the polymeric matrix) as well as the various porosities influences the effectiveness of the fifth catalysts. For the catalysts obtained by the using of the same chitosan/TEOS ratio in the synthesis gel the catalytic activity decreases in order: catalyst $C_3 >$ catalyst $C_2 >$ catalyst C_1 in agreement with the decrease of the number of active catalytic centers. In the case of the catalysts for which the ratio chitosan/TEOS was varied one notices an increase of catalytic activity with the increase of porosity (increasing of chitosan/TEOS ratio). The catalytic activity of catalyst C_5 is slightly higher than that of the catalyst C_4 as the increase of catalytic activity due to increase of porosity (catalyst C_5 versus catalyst C_4) is partially counterbalanced by the increase of the number of active catalytic centers (catalyst C_4 versus catalyst C_5).

Reusability of the catalyst

Recyclability is an important parameter in evaluating the effectiveness of heterogeneous catalysts. The reusability of catalyst C_3 was studied fifth times, including the use of the fresh catalyst. After each reaction the catalyst was separated, dried and then calcinated at 600°C for 4 h. A calcination step is required in order to regenerate the catalyst by eliminating of the adsorbed products that block the active catalytic sites. Variation of conversion in time after each use is plotted in figure 7.

As can be noticed from figure 7, the conversion values did not change after five uses of the catalyst. The results obtained are also confirmed by EDX analyses of catalyst C_3 carried out after the first reuse and respectively after the fourth reuse of the catalyst (table 6). EDX analysis performed after the first and the fourth reuse of the catalyst proved that there was no loss of metallic ions in the reaction mixture (table 6) and consequently the synthesized hard metallosilicate macrospheres are promising heterogeneous catalysts.

Table 6
CATALYST COMPOSITION AFTER THE FIRST AND THE FOURTH REUSE

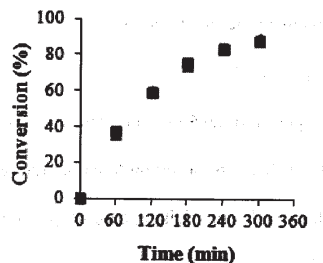


Fig. 7. Effect of catalyst C_3 reusability on the caprylic acid conversion: \checkmark - fresh catalyst (molar ratio caprylic acid : epichlorohydrin = 1.00:1.15; stirring speed 500 r.p.m.; 15 g catalyst/100 g reaction mixture; 85°C)

Conclusions

This work reports an original method for the obtaining of the hierarchical macrospherical metallosilicate catalysts. Due to their sizes and hardness these catalysts are easy to recover and to reuse. Metallosilicate microspheres (0.90 ÷ 1.10mm) with low silicon/metals ratios were easily synthesized at room temperature using chlorohydric acid as catalyst and tetraethyl orthosilicate as silicon source. Chitosan fulfilled both the role of shape generating agent as well as the role of template for the synthesized catalysts. The concentration of chitosan from the synthesis gel influences the porosity, the size and the shape of catalyst particles. For chitosan concentrations in the range 0.90 ÷ 1.35 perfectly shaped microspheres were obtained. Three starting silicon/metals molar ratios and three chitosan/TEOS ratios were used for the synthesis of catalysts. EDX analyses confirmed that metal ions were efficiently incorporated within the silica matrix. The synthesized catalysts were successfully tested in the esterification reaction of caprylic acid with epichlorohydrin.

References

- ZHU, K., EGEBLAD, K., CHRISTENSEN, C.H., *J. Inorg. Chem.*, **25**, 2007, p. 3955.
- WANG, L., ZHANG, Z., YIN, C., SHAN, Z., XIAO, F., *Micropor. Mesopor. Mater.*, **131**, no. 1-3, 2010, p. 58.
- ZHANG, B., DAVIS, S.A., MANN, S., *Chem. Mater.*, **14**, no. 3, 2002, p. 1369.
- YANG, Z., XIA, Y., MOKAYA, R., *Adv. Mater.*, **16**, no. 7, 2004, p. 727.
- LEE, Y.J., LEE, J.S., PARK, Y.S., YOON, K.B., *Adv. Mater.*, **13**, no. 16, 2001, p. 1259.
- DONG, A., WANG, Y., TANG, Y., REN, N., ZHANG, Y., YUE, Y., GAO, Z., *Adv. Mater.*, **14**, no. 12, 2002, p. 926.
- KUSTOVA, M., EGEBLAD, K., ZHU, K., CHRISTENSEN, C.H., *Chem. Mater.*, **19**, no. 12, 2007, p. 2915.

- EGEBLAD, K., CHRISTENSEN, C.H., KUSTOVA, M., CHRISTENSEN, C.H., *Chem. Mater.*, **20**, no. 3, 2008, p. 946.
- ZHANG, H., HARDY, G.C., KHIMYAK, Y.Z., ROSSEINSKY, M.J., COOPER, I., *Chem. Mater.*, **16**, no. 22, 2004, p. 4245.
- ZHANG, H., HARDY, G.C., ROSSEINSKY, M.J., COOPER, A.I., *Adv. Mater.*, **15**, no. 1, 2003, p. 78.
- TOSHEVA, L., MIHAILOVA, B., VALTCHEV, V., STERTE, J., *Micropor. Mesopor. Mater.*, **48**, no. 1-3, 2001, p. 31.
- TOSHEVA, L., VALTCHEV, V., STERTE, J., *Micropor. Mesopor. Mater.*, **35**, 2000, p. 621.
- KAIFENG, L., LEBEDEV, O.I., TENDELOO, G.V., JACOBS, P.A., PESCARMONA, P.P., *Chem. Eur. J.*, **16**, no. 45, 2010, p. 13509.
- ASAFTEI, I. V., BILBA, N., SANDU, I., *Rev. Chim. (Bucharest)*, **64**, no. 5, 2013, p. 509.
- ASAFTEI, I. V., BILBA, N., SANDU, I., *Rev. Chim. (Bucharest)*, **64**, no. 8, 2013, p. 836.
- SERANNO, D.P., GRIEKEN, R., MELGARES, A.M., MORENO, J.J., *Porous Mater.*, **17**, no. 2, 2010, p. 387.
- SAKTHIVEL, A., DAPURKAR, S.E., SELVAM, P., *Catal. Lett.*, **77**, no. 1-3, 2001, p. 155.
- Grieken, R., Escola, J.M., Moreno, J., Rodriguez, R., *Chem. Eng. J.*, **155**, no. 1-2, 2009, p. 442.
- AGUADO, J., CALLEJA, G., CARRERO, A., MORENO J., *Chem. Eng. J.*, **137**, no. 2, 2008, p. 443.
- SUBRAHMANYAM, C., LOUIS, B., RAINONE, F., RENKEN, A., VARADARAJAN, T.K., *Appl. Catal.*, **241**, no. 1-2, 2003, p. 205.
- IUPAC Recommendations Pure Appl. Chem., **57**, no. 4, 1985, p. 603.
- IUPAC Recommendations Pure Appl. Chem., **66**, no. 8, 1994, p. 1739.
- ENG-POH, NG, MINTOVA, S., *Microp. Mesop. Mater.*, **114**, no. 1-3, 2008, p. 1.
- PEPPER, K.W., *J. Appl. Chem.*, **1**, no. 3, 1951, p. 124.
- MURRAY, K.L., SEATON, N.A., DAY, M.A., *Langmuir*, **15**, no. 20, 1999, p. 6728.
- SEIDL, J., MALINSKY, J., DUSEK, K., HEITZ, W., *Adv. Polym. Sci.*, **5**, 1967, p. 113.
- DRAGAN, E.S., AVRAM, E., DINU, M.V., *Polym. Adv. Technol.*, **17**, no. 6, 2006, p. 571.
- SELVARAJ, M., KIM, B.H., LEE, T.G., *Chem. Lett.*, **34**, no. 9, 2005, p. 1290.
- SELVARAJ, M., SINHA, P.K., LEE, K., AHN, I., PANDURANGAN, A., LEE, T.G., *Microp. Mesop. Mater.*, **78**, no. 2-3, 2005, p. 139.
- AZIMOV, F., MARKOVA, I., STEFANOVA, V., SHARIPOV, K.H., *UCTM J.*, **47**, no. 3, 2012, p. 333.
- LIU, D., WEI, Y., YAO, P., JIANG, L., *Carbohydr. Res.*, **341**, no. 6, 2006, p. 782.
- SAKTHIVEL, A., BADAMALI, S.K., SELVAM, P., *Catal. Lett.*, **80**, no. 1-2, 2002, p. 73

Manuscript received: 11.02.2014